

Tissue-specific transcriptome analysis of drought stress and rehydration in *Trachycarpus fortunei* at seedling

Xiao Feng^{1,2,3,4}, Zhao Yang^{1,2,3,4} and Xiurong Wang¹

¹ College of Forestry, Guizhou University, Guiyang, Huaxi, China

² Institute for Forest Resources & Environment of Guizhou, Guizhou University, Guiyang, Huaxi, China

³ Key laboratory of Forest Cultivation in Plateau Mountain of Guizhou Province, Guizhou University, Guiyang, Huaxi, China

⁴ Key laboratory of Plant Resource Conservation and Germplasm Innovation in Mountainous Region (Ministry of Education), Guizhou University, Guiyang, Huaxi, China

ABSTRACT

Background: *Trachycarpus fortunei* has broad economic benefits and excellent drought resistance; however, its drought response, adaptation, and recovery processes remain unclear.

Methodology: In this study, the response, tolerance, and recovery processes of *T. fortunei* leaves and roots under drought stress were determined by Illumina sequencing.

Results: Under drought stress, *T. fortunei* reduced its light-capturing ability and composition of its photosynthetic apparatus, thereby reducing photosynthesis to prevent photo-induced chloroplast reactive oxygen damage during dehydration. The phenylpropanoid biosynthesis process in the roots was suppressed, *DHNs*, *LEA*, *Annexin D2*, *NAC*, and other genes, which may play important roles in protecting the cell membrane's permeability in *T. fortunei* root tissues. During the rehydration phase, fatty acid biosynthesis in *T. fortunei* roots was repressed. Weighted correlation network analysis (WGCNA) screened modules that were positively or negatively correlated with physiological traits. The real-time quantitative PCR (RT-qPCR) results indicated the reliability of the transcriptomic data.

Conclusion: These findings provide valuable information for identifying important components in the *T. fortunei* drought signaling network and enhances our understanding of the molecular mechanisms by which *T. fortunei* responds to drought stress.

Subjects Biochemistry, Molecular Biology, Plant Science, Forestry

Keywords *Trachycarpus fortunei*, Transcriptome, Drought stress, Rehydration, WGCNA

INTRODUCTION

Trachycarpus fortunei (Hook.) H. Wendl. (Fam.: *Palmae*; Gen.: *Trachycarpus*) is an evergreen tree that is widely distributed. It is an important economic and landscaping plant. The global climate is warming, the land area affected by water shortage is expanding, the frequency of droughts is increasing, and the severity and duration of droughts are increasing (Stocker *et al.*, 2014; Yao *et al.*, 2015; Lamaoui *et al.*, 2018). The drought stress

Submitted 16 July 2020
Accepted 21 January 2021
Published 1 April 2021

Corresponding author
Zhao Yang, zhy737@126.com

Academic editor
Yu Liang

Additional Information and
Declarations can be found on
page 15

DOI 10.7717/peerj.10933

© Copyright
2021 Feng et al.

Distributed under
Creative Commons CC-BY 4.0

OPEN ACCESS

experiment of 2-year-old *T. fortunei* from 19 provenances in Guizhou and Yunnan of China found that soluble sugar and Superoxide dismutase (SOD) reached the maximum value at 14 date, due to the difference in the ability of the provenances to resist drought, the lethality of seedlings reached 40% after rehydration of some provenances (Lan *et al.*, 2017). However, there is still a lack of research on the response and adaptation of *T. fortunei* to drought response.

Typical mechanisms for plants to resist drought include the development of vigorous root systems, the formation of epidermal wax, a thicker epidermal layer, regulation of stomatal conductance to reduce transpiration, elimination of reactive oxygen species, and activation of stress-related hormones. Under the pressure of drought environment, the leaves will close the stomata (Hummel *et al.*, 2010), and the cells will adjust the osmosis to increase the amount of free sugar and free amino acids (especially proline) (Showler, 2013). When it persists, the protein may lose its activity or become denatured, producing excess reactive oxygen species (ROS), stimulating the activity of oxidative stress kinases in leaf cells (Anjum *et al.*, 2011), photosynthesis is inhibited, leading to metabolic dysfunction and destruction of cell structure (Krasensky & Jonak, 2012; Li *et al.*, 2016). ROS are rapidly cleared due to various drought-induced signaling pathways regulated by abscisic acid (ABA) (Contreras-Porcia *et al.*, 2011). Productive ROS signaling requires both rapid increases in ROS, as well as the ability of cells to prevent ROS from reaching damaging levels through synthesis of antioxidants, including flavonols (Postiglione & Muday, 2020). ABA is a predominant hormone that regulates stomatal closure under drought stress. Plants recognize water deficit conditions in roots and that several molecular signals then move from roots to shoots (Takahashi *et al.*, 2020). CLAVATA3/EMBRYO-SURROUNDING REGION-RELATED 25 (CLE25) peptide transmits water-deficiency signals through vascular tissues, and affects ABA biosynthesis and stomatal control of transpiration in association with BARELY ANY MERISTEM (BAM) receptors in leaves (Takahashi *et al.*, 2018). ABA accumulation is enhanced mainly in the vasculature of the leaves, accumulated ABA is supposed to spread from the vasculature to all tissues to mediate stomatal movements and gene expression related to drought stress resistance (Kuromori, Seo & Shinozaki, 2018; Takahashi *et al.*, 2020), drought-responsive genes mainly involved photosynthesis, signal transduction, lipid metabolism, sugar metabolism, wax synthesis, cell wall regulation, osmotic adjustment (Chen *et al.*, 2020). When the damage exceeds a certain level, it will cause plant plastic damage, growth retardation, or even death. So far, little is known about the regulation during the stress response process of *T. fortunei*, and the dynamic changes of genes when *T. fortunei* reaches severe drought are still unknown.

The acquisition of full-sibling progeny is to retain the excellent traits of the family through sexual crossing, with the same genetic background, eliminating the influence of different genotype differences within the species. The dynamic changes of physiological indicators are the products of differential gene expression, and the tolerance to drought is a complex phenotypic trait controlled by multiple genes. Transcriptomics analysis is used to identify genes that play an important role in drought tolerance and infer the main mechanisms involved (Li *et al.*, 2017). At present, there is a lack of *T. fortunei* genome and

transcriptome data, and relevant information is not available. In order to understand the molecular resistance and recovery mechanisms of *T. fortunei*, through the simulation of natural drought stress process at seedling stage, the expression profile changes of related resistance genes were obtained, combined with phenotypes and physiological indicators to evaluate the molecular response of *T. fortunei*.

MATERIALS AND METHODS

Test

In April 2017, we conducted a *T. fortunei* germplasm survey and selected excellent male and female plants for hybridization, the excellent paternal pollen collected in Guiding, Guizhou province, China, was sexually crossed with the excellent female plants in Huaxi, Guizhou province, China. The full-sibling progeny were obtained. The full-sibling progeny of 1.5-year-old seedlings was selected for transplanting and placed in a greenhouse (Normal growth 4 months after transplanting). The soil type in the pot was humus: yellow soil (1:3). Natural drought stress was simulated and all plants were normally irrigated for 3 days before drought treatment. After the irrigation was stopped, sampling was conducted between 8:00–9:00 in the morning, leaves and root tips were collected every three days from new plants (some leaves were immediately frozen in liquid nitrogen for transcriptome sequencing and RT-qPCR, while others were used for biochemical parameters measurements), phenotypic changes were also recorded. The leaf collection site was unified into mature healthy leaves, root tips were collected from the roots. Samples were collected every 3 days until the fresh leaves of the seedlings were extremely atrophic. A total of 15 days between the cessation of irrigation and the end of the severe drought. At this point, drought stress concluded and the rehydration experiment was conducted, rehydration was performed on the same day to the control (0d) level. After 12 h (Re0.5d), 1 day (Re1d), 3 days (Re3d), and 6 days (Re6d), rehydration and related indicators were measured. The aluminum box soil drying method was used to determine the soil absolute moisture content (AMC). A leaf area scanner was used to measure the *T. fortunei* leaf area.

Test methods

Determination of biochemical parameters

First, mature leaves and root tips were collected. Using the methods described in *The Principle and Technology of Plant Physiology and Biochemistry Experiment Book* (Xuekui, 2006) to determine the following indicators. The proline (Pro) content in the leaves were determined according to the method of acid ninhydrin colorimetry (Demirel *et al.*, 2020). The level of Malondialdehyde (MDA) content in the leaves (Ml) and roots (Mr) were determined by Thiobarbituric acid (TBA) method (Liu, Wei & Li, 2014). Leaf superoxide dismutase (SOD) activity was measured spectrophotometrically at 560 nm using the inhibition of photochemical reduction of nitro-blue tetrazolium (NBT) in the presence of riboflavin under light according to Giannopolitis & Ries (1977). Root activity (Rv) in the roots was determined using triphenyltetrazolium chloride (TTC) method. Peroxidase (POD) activity was determined using the phenol method. The experiment

included 3 biological and technical replicates. The statistics and analysis of physiological related data are performed using R software (<https://www.r-project.org/>), Cluster analysis of the samples was performed using ggtree software package (Yu *et al.*, 2017). A principal components analysis (PCA) was performed using FactoMineR software package (Le, Josse & Husson, 2008).

Transcriptome material collection and library construction

The material selection time nodes included 0 d (start drought), 9 d (ninth day of drought), 15 d (15th day of drought), Re0.5d (twelfth hour after rehydration), and Re1d (the first day/24 h after rehydration), collect the roots tips and mature leaves of the above time nodes, each with three biological replicates. The leaf collection site was unified into mature healthy leaves. Root tips were collected from the roots, washed with distilled water, wrapped in tin foil, and stored in liquid nitrogen. The isolation of total RNA from above samples were isolated according to the instruction manual of the Trizol Reagent (Invitrogen, Carlsbad, CA, USA). Nandrop 2000 (Thermo Fisher Scientific, Waltham, MA, USA) was used to determine the concentration and purity of the RNA. The RNA integrity was assessed by agarose gel electrophoresis while its integrity number (RIN) value was measured by Agilent 2100 (Agilent Technologies, Santa Clara, CA, USA). After the quality of the total RNA sample met the requirements (with at least 1µg sample of concentration ≥ 50 ng/µL, OD_{260/280} = 1.8–2.2), the mRNA was enriched with Oligo (dT) magnetic beads. Further, the mRNA was added with fragmentation buffer and cut into short fragments. Using mRNA as templates, cDNA was reverse transcribed using six-base random primers. The double-stranded cDNA samples were purified, end-repaired, added with poly(A) tails and then ligated to the sequencing adapters to create cDNA libraries. After the libraries passed quality test, they were sent to Shanghai Ouyi Co. (Shanghai, China) for sequencing from both ends with an Illumina HiSeq X Ten machine.

Data processing and analysis

Raw data were quality filtered and reads with adapters or poor-quality sequences were removed using the Trimmomatic tool (Bolger, Lohse & Usadel, 2014). Assembly of the reads was performed using the Trinity (Grabherr *et al.*, 2011) software paired-end to get the assemblage of the transcripts and unigene libraries. Diamond (Buchfink, Xie & Huson, 2015) was used to compare the unigenes to the NCBI NR, EuKaryotic Orthologous Groups (KOG), Gene Ontology (GO), Swiss-Prot, eggNOG, and Kyoto Encyclopedia of Genes and Genomes (KEGG) databases. Functional analyses were conducted using the HMMER comparison of unigenes to the Pfam database (Mistry *et al.*, 2013).

The PlantTFDB database (Jin *et al.*, 2013) was used to identify transcription factors (TFs).

Using Bowtie2 (Langmead & Salzberg, 2012), the number of unigene reads in each sample was obtained. The expression of unigene Fragments Per Kilobase of transcript per Million Mapped reads (FPKM) was calculated using eXpress (Roberts, 2013). First, the correlation heatmap and PCA analysis were performed using the expression levels of all samples, followed by PCA analysis for different tissue samples, roots and leaves.

Use DESeq (Anders & Huber, 2012) software to standardize the number of Unigene counts

in each sample (basemean value is used to estimate expression), calculate the difference multiple, and use NB (negative binomial distribution test) to test the difference reads significance, and finally screen differentially expressed gene (DEG) according to the difference multiple and the difference significance test results. DEG screening threshold was set to $p < 0.05$ and $|\text{foldchange}| > 2$. The clusterProfiler package was used to perform GO and KEGG enrichment of the DEGs (Yu et al., 2012). GOSemSim was used to calculate the similarity between GO terms (Yu et al., 2010). GO term similarity clustering was conducted using ggtree. Calculation results were selected if $q < 0.01$ in order to avoid the very general sets and limit the annotation of >300 genes and GO terms of <100 genes. According to the p -value screening, the top 10 KEGG pathways were used to map multiple sets of enriched analysis bubbles. Short Time-series Expression Miner (STEM) software was used to perform the trend cluster analysis (Ernst & Bar-Joseph, 2006), which was divided into five stages according to the time of occurrence; the combination of different stages of combined genes was input and normalized. The number of models was set to 50.

Screening for the top 5,000 genes of the leaf and root gene expression matrix (background gene set for all genes) was conducted according to the median absolute deviation (MAD) method. A matrix of the relationship between gene expression and sample traits was established using the weighted co-expression network analysis (WGCNA) package (Langfelder & Horvath, 2008), which was subsequently transformed into a leader matrix to construct a joint analysis of the modules and traits.

Nine genes were selected to validate the transcriptome data using real-time quantitative PCR (RT-qPCR). SuperMix was removed and cDNA was synthesized using TransScript One-Step gDNA. The first strand of the cDNA fragment was synthesized from total RNA. RT-qPCR was performed on a real-time CFX96 Touch PCR instrument. The PCR reaction conditions were as follows: preheating at 95 °C for 30 s, 40 cycles of heat denaturation at 95 °C for 5 s, and annealing at 60 °C for 34 s. The *T. fortunei* actin gene was used as the reference gene for data standardization. Each sample was repeated three times and the relative expression levels were calculated using the $2^{-\Delta\Delta Ct}$ method (Schmittgen & Livak, 2008). The primer sequences used in this study are provided (Table 1).

RESULTS

Plant-related physiological and biochemical indicators

During the experiment, leaves entered the folded state after 9 d (Fig. 1A), AMC decreased continuously from 0 to 15 d (Fig. 1B). After 9 d, the POD activity reached its maximum value (Fig. 1C), while SOD activity was at its lowest value (Fig. 1D). After 12 d, the leaves were folded and curled, leaf area decreased (Fig. 1E), and the MDA content in the roots increased to its maximum value (Fig. 1F), and the MDA content in the leaves reached its maximum value in Re0.5d (Fig. 1G), but was delayed compared to the roots. The Pro content in the leaves reached its maximum value (Fig. 1H). After 15 d, SOD activity reached its peak value, and Rv (Fig. 1I) and area decreased to their lowest values. Each indicator showed a correlation with the positive/negative modes of stress, Area was positive correlation with Rv (Correlation coefficient = 0.70, $P = 1.918869e-05$ (***)),

Table 1 The primer sequences used in this study. PCR primer sequences.

No.	Gene_ID	Forward primer	Reverse primer	Product length (bp)	gene_name
	Reference Gene	5' TGAATCTGGTCCATCCATTGTC 3'	5' AGAACATAACCATAACCAAGCTC 3'	60	Actin
1	TRINITY_DN53033_c0_g1_i1	5' ACCCTCCATCTCAGCCTTCA 3'	5' TGCCTCTGTGACCTCCTTTC 3'	146	accA
2	TRINITY_DN46177_c1_g1_i1	5' TGTCCTATGTGCCTAGCAGTAA 3'	5' TCCGCATCCAACAATGTAAGAG 3'	76	Annexin D2
3	TRINITY_DN35842_c0_g1_i2	5' GACTGCTACTACGTCCCAACCTG 3'	5' CGACAAACCAATGGCTTCTTCA 3'	81	cytochrome P450
4	TRINITY_DN51483_c1_g1_i2	5' ATCAGGTCACCGTCCATAGC 3'	5' TTCTCCTTCAATCCCTTCTTTT 3'	169	Dehydrin COR410
5	TRINITY_DN52956_c0_g1_i2	5' ATAGGATTTGGCAGATAGCATTG 3'	5' AACGCCTTCCATACCGCACT 3'	64	KCS-11
6	TRINITY_DN48903_c0_g2_i1	5' ACTTGCTAAGCCAGCCATTC 3'	5' AATCCCTTTGATGCCACTCC 3'	245	NAC 47
7	TRINITY_DN58051_c0_g2_i12	5' TGTTGGCATCGTCTCAACT 3'	5' AATGAATGCACGGTTTGA 3'	87	P5CS
8	TRINITY_DN57760_c0_g1_i2	5' TGCTGGAAAGAGTTAGAAGAGG 3'	5' AGATTCGATATTATGGGTGGC 3'	62	PRODH
9	TRINITY_DN27793_c0_g1_i1	5' ATGGCAACCTTCCACTTCTCTG 3'	5' ACCAACTGATCCGAGCACTCCTT 3'	116	YLS3

Area and Pro show negative correlation (Correlation coefficient = -0.83 , $P = 1.062141e-08$ (***)) (Fig. 1J). Samples of 12d and 15 d were clustered into member 2 (Fig. 1K). After rehydration, most *T. fortunei* gradually stretched at Re0.5d. PCA of physiological indexes showed that PC1 on the X axis captures the greatest variation and accounts for 50.1% of the total variance around the PCs whilst PC2 on the Y axis captures the second greatest variation and accounts for 25.4% of the total variance around the PCs (Fig. 1L), the PCA results revealed that Re6d and 0 d were closer and coercion was lifted.

Data quality control, splicing, comparison, expression quantification, and differential analysis

The raw data of each sample (Q30) ranged from 96.88% to 97.57%. The effective data ranged from 6.98 to 7.18 G. The average GC content was 47.94%. The four base content distribution of each sample was relatively uniform. A total of 66,270 unigenes were spliced with a total length of 55,575,529 bp and an average length of 840. In total, 43,238 (65.25%) unigenes were annotated in the NCBI NR database, while 30,054 (45.35%) unigenes were annotated in the Swiss-Prot database. A total of 51,381 CDS sequences were predicted, of which, 43,373 were predicted by the database comparison method and 8,008 were predicted by ESTScan. A total of 15,696 unigene annotations were identified in the TF database and were distributed across 58 families. The raw data were stored in the NCBI/SRA database (BioProject accession No.: [PRJNA598974](https://www.ncbi.nlm.nih.gov/bioproject/PRJNA598974)), this transcriptome Shotgun Assembly project has been deposited at DDBJ/EMBL/GenBank under the accession [GIYF00000000](https://www.ncbi.nlm.nih.gov/nuccore/GIYF00000000).

The distance clustering heatmap between the samples revealed that the samples were reproducible and the leaf and root tissues were distinct (Fig. 2A). PCA revealed that the repeatability was better among groups and the cumulative contribution rate was high, PC1 on the X axis captures the greatest variation and accounts for 29.69% of the total variance around the PCs whilst PC2 on the Y axis captures the second greatest variation

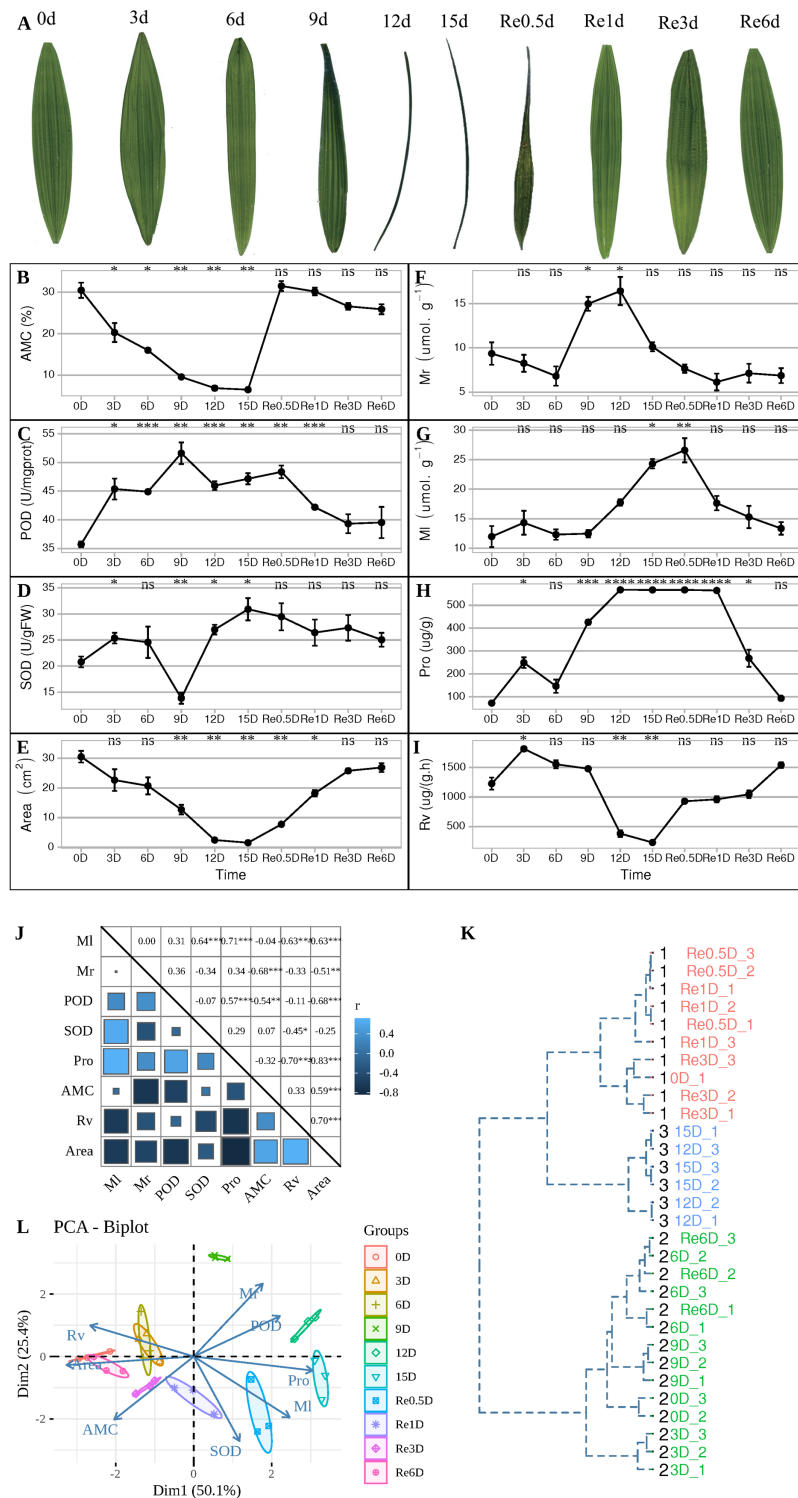


Figure 1 During the experiment, leaves entered the folded state after 9 d (Fig. 1A). Changes in the physiological indicators of *T. fortunei* during drought stress and rehydration. (A) Collection of *T. fortunei* leaf samples during the experiment; (B) changes in the absolute moisture content of the soil; (C) changes in the POD of *T. fortunei* leaves; (D) changes in the SOD activity of the leaves; (E) changes in the area of *T. fortunei* leaves; (F) changes in the MDA content of the roots; (G) changes in the MDA content of the roots; (H) changes in the Pro content of the leaves; (I) changes in the root activity tetrazolium reduction

Figure 1 (continued)

intensity; (J) correlation of the indices during stress; (K) cluster analysis of the samples during stress; (L) PCA of the physiological indexes during stress. In (B–I), the unpaired Welch's *t*-test was done using the R-function *t*test. An asterisk (*) indicates that there is difference compared with the "0d" group, **p* < 0.05, ***p* < 0.01, ****p* < 0.001, and "ns" means no difference, the error line represents the standard deviation error; the square size. In (K), the distance matrix was run with hclust, and a dendrogram was plotted that displays a hierarchical relationship among the samples. (J) Represents the correlation value, and the asterisk (*) represents the significance of correlation; members represent members grouped together.

Full-size  DOI: 10.7717/peerj.10933/fig-1

and accounts for 9.56% of the total variance around the PCs, samples of leaves and roots are closely grouped together, which is related to tissue specificity (Fig. 2B). PCA analysis of the leaves (Fig. 2C) and roots (Fig. 2D) revealed that the samples of the leaves in each time group were more clearly separated, which may indicate that the leaves responded more to the drought than the roots. After screening for DEGs, compared to 0d_L (Fig. 2E), the DEGs of the corresponding parts of each stage included 4,791 (9 d), 9,108 (15 d), 5,480 (Re0.5d), and 3,211 (Re1d) DEGs. Compared to 0d_R (Fig. 2F), the DEGs of the corresponding parts of each stage included 7,995 (9 d), 8,556 (15 d), 4,968 (Re0.5d), and 6,204 (Re1d) DEGs. After 15 d, the number of DEGs reached its peak value compared to 0 d. The five differential combinations between the L and R sites had a total difference of 11,510 DEGs (Fig. 2G), which were associated with tissue specificity.

Functional enrichment analysis of DEGs

The GO similarity enrichment (BP category) revealed that the leaf responses to hormones were active in the L1 group (Fig. 2H). In the L2 group, photosynthesis (ko00195), photosynthesis-antenna proteins (ko00196), and porphyrin and chlorophyll metabolism (ko00860) were the most enriched terms (Fig. 2I). Most of the DEGs in the pathway were downregulated in 15d_L. The light-harvesting complex I chlorophyll a/b binding protein 1-5 (*Lcha1-5*) and *Lhcb1-7* were lowered in 15d_L.

The biosynthesis of metabolites in the roots was enriched in the R2 group (Fig. 2I). In the R2 group, the most significantly enriched pathway included phenylpropanoid biosynthesis (ko00940), and most of the ko00940 DEGs were downregulated in 15d_R. In the R1, R3, and R4 groups, fatty acid biosynthesis (ko00061) and fatty acid metabolism (ko01212) were enriched.

The recovery of plant phenotypes was rapidly developed after rehydration. In the 15d_L/Re0.5d_L group, photosynthesis-related genes were activated, and *Lca1-5* and *Lcb2-6* were upregulated in Re0.5d_L. In the R3 group, fatty acid biosynthesis (ko00061)-related DEGs were all downregulated in Re0.5d.

The STEM analysis revealed that there were 16 significantly different modules in the leaf group (Fig. 3A), profile 23 (0.0, 0.0, -1.0, 1.0, 1.0) (Fig. 3D), and profile 10 (0, -1, -2, -1, 0) (Fig. 3C), which all dropped to their lowest values after 15 d. In profile10, photosynthesis (ko00195), photosynthesis-antenna proteins (ko00196), carbon fixation in photo, and synthetic organisms (ko00710) were enriched. Profile43 (0.0, 1.0, 3.0, 3.0, 2.0)-related gene expression increased to its maximum value after 15 d (Fig. 3G). Starch and sucrose metabolism (ko00500) and diterpenoid biosynthesis (ko00904) were enriched

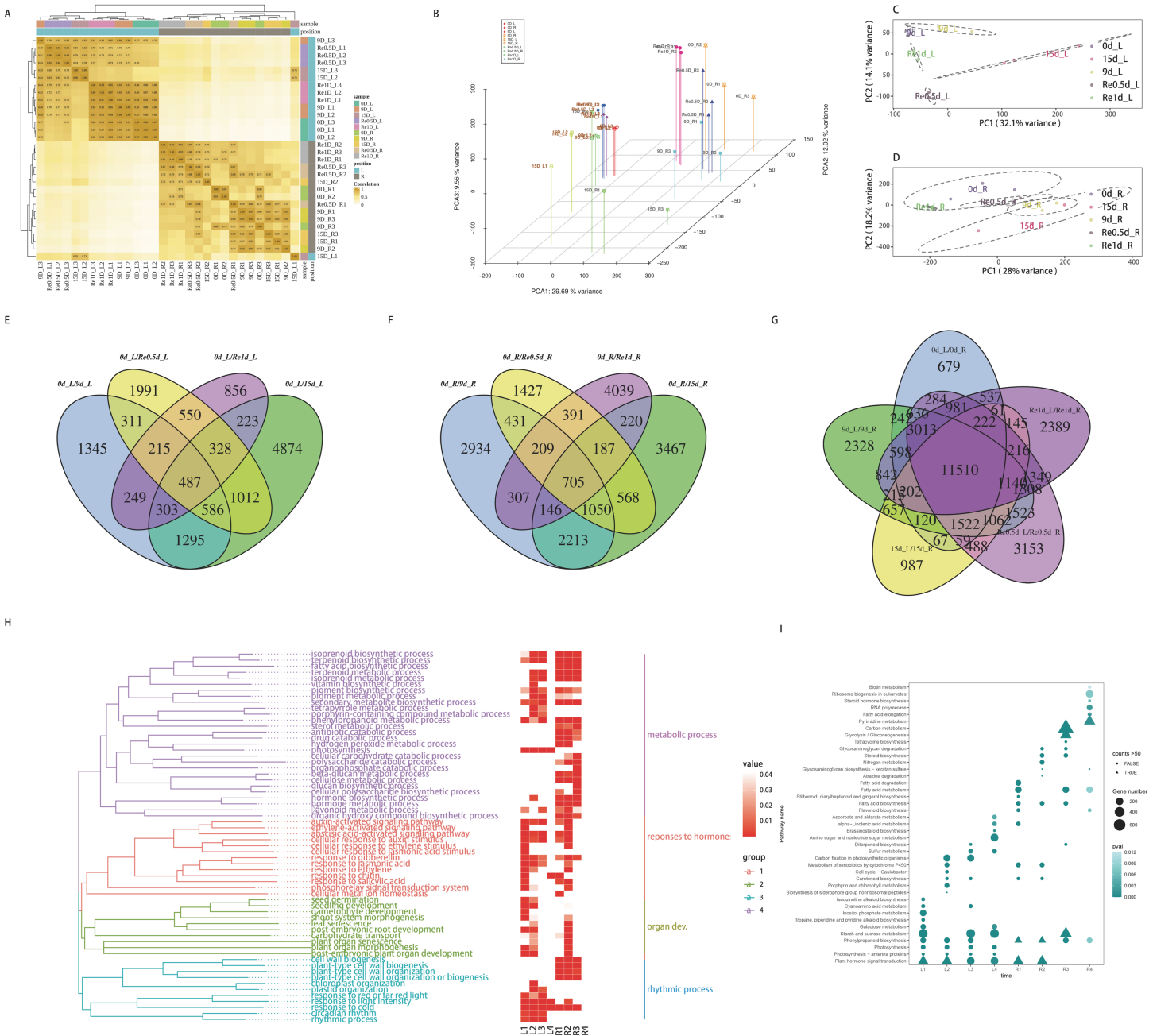


Figure 2 Analysis of transcriptome data and functional enrichment of differentially expressed genes. (A) Heatmap of the correlation of sample gene expression; (B) three-dimensional PCA; (C) leaf PCA; (D) root PCA; (E) Venn diagram of DEGs in different leaf combinations; (F) Venn diagram of DEGs in different root combinations; (G) Venn diagram of DEGs between the leaves and roots at different time periods; (H) GO enrichment similarity clustering and heatmap; (I) KEGG top 10 bubble chart. Full-size [DOI: 10.7717/peerj.10933/fig-2](https://doi.org/10.7717/peerj.10933/fig-2)

in Profile43. Profile25 (0.0, 0.0, 0.0, -1.0, 1.0) and profile 36 (0.0, 1.0, 1.0, -1.0, 1.0)-related gene expression were reduced to their lowest values in Re0.5d (Figs. 3E and 3F).

Arachidonic acid metabolism (ko00590) and linoleic acid metabolism (ko00591) were enriched in profile25. Fatty acid biosynthesis (ko00061) and fatty acid elongation (ko00062) were enriched in profile36.

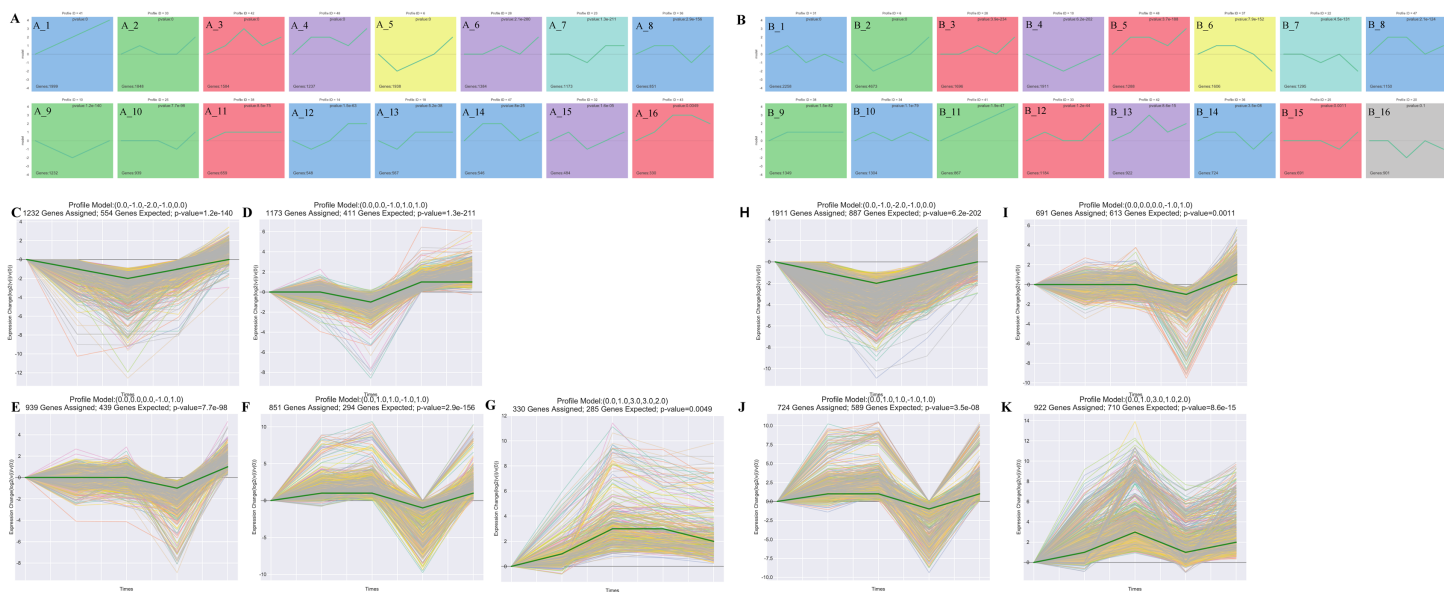


Figure 3 Cluster analysis of the gene expression trends during *T. fortunei* drought. (A) Time-series analysis significance module of the leaves during drought stress; (B) time-series analysis significance module of the roots during drought stress; (C–G) selected significant leaf profiles (C) profile10, (D) profile23, (E) profile25, (F) profile36, (G) profile43; (H–K) selected significant root profiles (H) profile10, (I) profile25, (J) profile36, (K) profile42. [Full-size !\[\]\(1663bb69f307a960345edb0e712f8c02_img.jpg\) DOI: 10.7717/peerj.10933/fig-3](https://doi.org/10.7717/peerj.10933/fig-3)

There were 15 significant differences in the root group (Fig. 3B). Profile10 (0.0, –1.0, –2.0, –1.0, 0.0)-related gene expression reached its lowest value after 15 d (Fig. 3H). Phenylpropanoid biosynthesis (ko00940) and glycosaminoglycan degradation (ko00531) were enriched in Profile10. Profile42 (0.0, 1.0, 3.0, 1.0, 2.0)-related gene expression peaked after 15 d (Fig. 3K), at which point, linoleic acid metabolism (ko00591), cutin, suberine, and wax biosynthesis (ko00073), and sulfur metabolism (ko00920) were enriched. In Profile25 (0.0, 0.0, 0.0, –1.0, 1.0), fatty acid biosynthesis (ko00061) was enriched (Fig. 3I). Profile36 (0.0, 1.0, 1.0, –1.0, 1.0)-related gene expression reached its lowest values in Re0.5d (Fig. 3J). Starch and sucrose metabolism (ko00500) and galactose metabolism (ko00052) were also enriched in Profile36.

Weighted correlation network analysis

The Weighted correlation network analysis (WGCNA) revealed that the leaves divided into 14 modules and the roots divided into 11 modules. In the leaf co-expression analysis network (Fig. 4A), the lightcyan1 module was significantly positively correlated with M1 (Correlation coefficient = 0.77, $P = 8e-04$), darkturquoise module was significantly positively correlated with M1 (Correlation coefficient = 0.89, $P = 1e-05$) and POD (Correlation coefficient = 0.9, $P = 6e-06$), the black module was significantly negatively correlated with M1 (Correlation coefficient = –0.56, $P = 0.03$), and the brown4 module was correlated with rehydration stress expression after 15 d in Re0.5d (Fig. 4B). The GO enrichment analysis (CC category) revealed that the brown4 module was associated with thylakoid (GO:0009579) and chloroplast thylakoid (GO:0009534) (Fig. 4C_3). The brown module was significantly positively correlated with area (Correlation coefficient = 0.63,

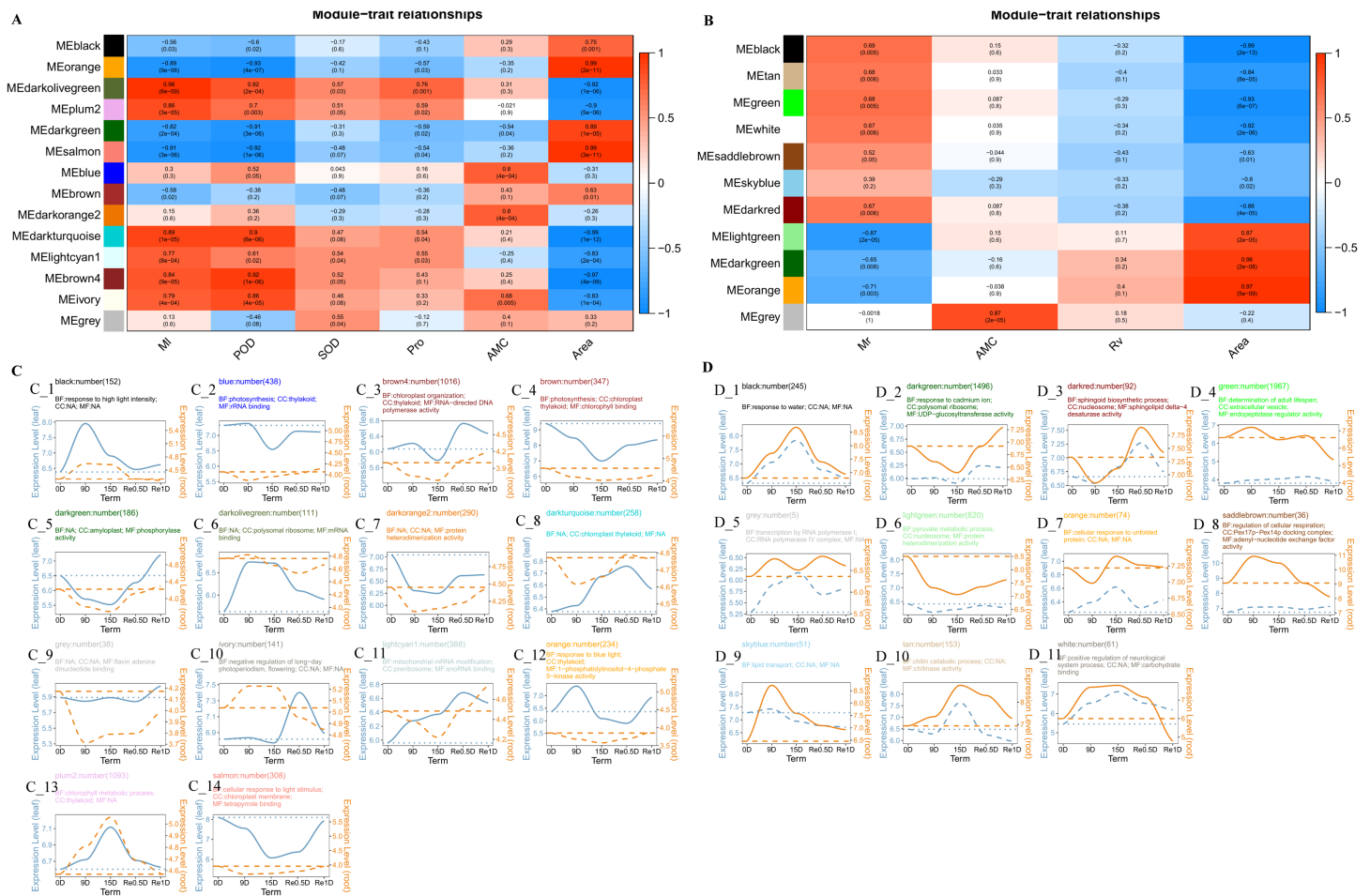


Figure 4 Analysis of the co-expression networks. (A) Leaf trait and module correlation map; (B) different module gene expression patterns in the leaf; (C) root trait and module correlation map; (D) different module gene expression patterns in the roots. Note: B and D represent the expression trend of genes in the lower leaves and roots of different modules (the average of all genes in the module was normalized and linearly fitted); the left of the double axis is the tick mark (“# 6B9EC2”) that represents the leaves; the right of the double axis is the tick mark (“# EE861A”) that represents the roots; the text includes the number of gene modules, module names, and GO enrichment analysis results (displayed with the smallest p-value for each of BP, CC, and MF category); The gene trends in the module are processed by taking the logarithm of the gene expression in the module, and fitted in a linear simulation.

Full-size [DOI: 10.7717/peerj.10933/fig-4](https://doi.org/10.7717/peerj.10933/fig-4)

$P = 0.01$). Additionally, the GO enrichment analysis (CC category) indicated that chloroplast thylakoid and plastid thylakoid (GO:0031974) were enriched (Fig. 4C₄). The darkorange2 module and AMC were significantly positively correlated (Correlation coefficient = 0.8, $P = 4e-04$), protein heterodimerization activity (GO:0046982) was enriched (MF category) (Fig. 4C₇).

In the root co-expression analysis network (Fig. 4B), the black module was significantly negatively correlated with area (Correlation coefficient = -0.99 , $P = 2e-13$). Response to water (GO:0009415), response to cold (GO:0009409), and response to salt stress (GO:0009651) (BP category) were enriched (Fig. 4D₁). *DHNs* *COR410-like* (TRINITY_DN51483_c1_g1_i2), *LEA14* (TRINITY_DN41505_c0_g2_i2), *NAC 47* (TRINITY_DN48903_c0_g2_i1), and *Annexin D2* (TRINITY_DN46177_c1_g1_i1) aggregated in response to water (GO:0009415). The light green module was significantly

positively correlated with area (Correlation coefficient = 0.87, $P = 2e-05$). Protein heterodimerization activity (GO:0046982), water transmembrane transporter activity (GO:0005372), and water channel activity (GO:0015250) (CC category) were enriched (MF category) (Fig. 4D_6).

Real-time quantitative PCR results

The RT-qPCR results revealed that TRINITY_DN53033_c0_g1_i1 (ACCA, Fig. 5A) in roots and leaves showed a significant down-regulated expression at Re0.5d (Compared to 0d); TRINITY_DN46177_c1_g1_i1 (*Annexin D2*, Fig. 5B), TRINITY_DN51483_c0_g1_i2 (*Dehydrin COR410*, Fig. 5D), TRINITY_DN48903_c0_g2_i1 (*NAC47*, Fig. 5F) showed up-regulated expression in roots at 15d (Compared to 0d) Log_2 ($^{\text{Fold change}}$) and log_2 ($2^{-\Delta\Delta\text{Ct}}$) were subjected to linear correlation analyses (Fig. 5J). Results revealed a positive correlation (0.79) with the RNA-Seq results ($R^2 = 0.65$). Thus, the RT-qPCR and RNA-Seq data were relatively consistent.

DISCUSSION

Drought is one of the main abiotic stressors affecting plant growth and development. Drought responses may vary in different plant organs or tissue and the analysis in both mature leaves and root tips is critical for plants to adapt to water deficits (Feng et al., 2017). After entering the drought state, *T. fortunei* leaves fold, root activity continuously decreases, Pro activity continuously increases, and the genes related to photosynthesis (ko00195) and photosynthesis-antenna proteins (ko00196) are continuously downregulated (0, -1, -2, -1, 0). Under drought stress, the light absorption of antenna proteins decreases, electron transport rates of PSII and PSI decreases, ROS accumulation increases, photosynthetic pigments are destroyed, RAC activity decreases (Din et al., 2011; Sharma et al., 2012; Guo et al., 2017; Dalal & Tripathy, 2018; Luo et al., 2018; Michaletti et al., 2018). Resuscitation plants are able to survive 95% of their cell water loss, one tolerance mechanism is to reversibly shut down photosynthesis, for example, in *Xerophyta humilis*, *psbR*, *psbA*, and *psbP* were downregulated during dehydration, and complex water regulation expression trends were exhibited (Dace et al., 1998; Collett et al., 2003). In this study, under drought stress, the expression of chlorophyll a-b binding proteins decreased and the synthesis of photosynthesis-related factors decreased. After rehydration, RAC and other photosynthetic-related genes were activated and recovered to a relatively consistent level after 0 d in Re1d. Gene expression of the thylakoid-associated cellular components proliferated after rehydration (Fig. 4C_3, brown4). *T. fortunei* *Psb O*, *Psb P*, *Psb Q*, *Psb R*, and other PSII subunits were downregulated under drought stress and gradually increased after rehydration. *T. fortunei* also reduced its light-trapping ability and the composition of the photosynthetic apparatus, thereby reducing photosynthesis and increasing drought resistance by leaf folding to prevent light-induced chloroplast ROS damage due to dehydration.

Plant roots may induce specific stress responses to cope with the early perception of soil water loss (Haas et al., 2019). MDA is a product of membrane lipid peroxidation that is produced when plants are under stress, and the content of MDA can reflect the degree of

cell membrane damage (Dong et al., 2019). The MDA content in the root reaches its peak at 12d, which is faster than the time node of the highest MDA value in the leaf (Figs. 1F and 1G) In the R2 group, phenylpropanoid biosynthesis (ko00940) was curbed, most of the DEGs (48/53) were downregulated in 15d_R, and some genes (27) of profile10 (0.0, -1.0, -2.0, -1.0, 0.0) were expressed. Protein phosphorylation and dephosphorylation are important signaling events that lead to drought tolerance (Deeba, Pandey & Pandey, 2016). ABA signaling is majorly composed of three core components: ABA receptor, protein kinases, and protein phosphatases (Saini, Singh & Pandey, 2020). PP2C belongs to a group of phosphatases involved in ABA signaling and is a negative regulator (Zhang & Gan, 2012). After ABA, polyethylene glycol and dehydration treatments, the accumulation rate of *OsPP2C09* (*Oryza sativa* L.) transcripts in roots was more rapid and greater than that in shoots (Zhang et al., 2020). Both PP2C-related DEGs in L2 and R2 groups were upregulated after 15 d. In order to absorb water and survive under drought stress, various organic solutes accumulate in the cytoplasm and chloroplasts for osmotic adjustment (Rajasheker et al., 2019). ABA can induce the accumulation of intracellular osmoprotectants, such as the LEA post-embryonic protein, chaperone proteins, carbohydrates, and Pro, which may be critical for survival under drought stress (Wang et al., 2018). The relationship between water transmembrane transporter activity (GO:0005372) and water channel activity (GO:0015250) was positively correlated with area (Fig. 4D_6, lightgreen), the black module was significantly negatively correlated (Fig. 4B), and the expression of DHNs was generally regulated and induced by ABA, which can reduce root water conductivity (Choi, Zhu & Close, 1999; Hand et al., 2011; Li et al., 2019a). LEA proteins bind to a large number of water molecules and maintain normal metabolism in cells (Ingram & Bartels, 1996). In a previous study, rice *OsANN3* was found to mediate Ca^{2+} influx by binding to phospholipids, and overexpression significantly increased drought stress survival (Li et al., 2019b). *DHNs* *COR410-like* (TRINITY_DN51483_c1_g1_i2), *LEA14* (TRINITY_DN41505_c0_g2_i2), *NAC 47* (TRINITY_DN48903_c0_g2_i1), and *Annexin D2* (TRINITY_DN46177_c1_g1_i1) aggregated in response to water (GO:0009415) term which is enriched in root black modules (Fig. 4D_1). qRT-PCR showed *Annexin D2* (Fig. 5B), *Dehydrin COR410* (Fig. 5D), *NAC47* (Fig. 5F) upregulated in roots at 15d. As drought persisted, phenylpropanoid biosynthesis in the roots was suppressed, the *DHNs*, *LEA*, *Annexin D2*, *NAC*, and other genes were expressed, possibly to protect cell membrane permeability in *T. fortunei* root tissues.

Resilience is an important physiological feature of drought-tolerant genotypes. The ability to preserve tissue health, integrity, and avoid aging is vitally important. Resurrection plants may have pathways that inhibit drought-related senescence (Rivas et al., 2016; Challabathula, Zhang & Bartels, 2018; Griffiths, Gaff & Neale, 2014). The biosynthesis of palmitic (C16:0), linoleic (C18:2), linolenic (C18:3) and stearic acid (C18:0) increased 18, 12, 20, and 8-fold during dehydration in *Pleopeltis polypodioides*, rehydration lowered levels of peroxides, the activity of glutathione-oxidizing enzymes, and fatty acids (John & Hasenstein, 2018). After *T. fortunei* rehydrated for 12 h, the leaves gradually recovered from the fully folded state. In profile36 (0.0, 1.0, 1.0, -1.0, 1.0),

fatty acid biosynthesis (ko00061) (TRINITY_DN53033_c0_g1_i1; TRINITY_DN67658_c0_g1_i1) was enriched in the leaves. Meanwhile, in root profile25 (0.0, 0.0, 0.0, -1.0, 1.0) (Fig. 3B), the fatty acid biosynthesis (ko00061) (TRINITY_DN48458_c0_g1_i1; TRINITY_DN52213_c0_g1_i2; TRINITY_DN53033_c0_g1_i1) pathway was simultaneously enriched. The transcripts of fatty acid biosynthesis (TRINITY_DN53033_c0_g1_i1; TRINITY_DN67658_c0_g1_i1) were annotated as ACCase subunit alpha (acetyl-coenzyme A carboxylase carboxyl transferase subunit alpha, chloroplastic), whose transcripts (TRINITY_DN52213_c0_g1_i2) encoded stearyl-ACP desaturase (SAD). ACCase is a key, rate-limiting enzyme involved in fatty acid biosynthesis that catalyzes the carboxylation of acetyl-CoA to form malonyl-CoA, providing a substrate for the synthesis of fatty acids and many secondary metabolites (Rajasekharan & Nachiappan, 2010). Fatty acid is the main component of cell and organelle membrane lipids. The regulation of membrane lipid contents and compositions is an effective regulation method for adapting to drought conditions, as well as a positive regulation mechanism during recovery after rehydration (Liu & Tingting, 2018). In the R3 group, fatty acid biosynthesis (ko00061)-related DEGs were downregulated in Re0.5d and some genes in profile25 (0.0, 0.0, 0.0, -1.0, 1.0) were expressed in the roots. Additionally, α -CT reached its lowest expression level in Re0.5d. This indicated that fatty acid biosynthesis in *T. fortunei* roots is repressed during the rehydration phase after extreme drought.

CONCLUSIONS

Under drought stress, *T. fortunei* reduces its light-trapping ability and the composition of the photosynthetic apparatus, thereby reducing photosynthesis and increasing drought resistance by leaf folding to prevent light-induced chloroplast ROS damage to dehydration. As drought conditions worsen, phenylpropanoid biosynthesis in the roots is suppressed, *DHNs*, *LEA*, *Annexin D2*, *NAC*, and other genes that may protect the cellular membrane's permeability in *T. fortunei* root tissues. Fatty acid biosynthesis in *T. fortunei* roots is repressed after rehydration.

ADDITIONAL INFORMATION AND DECLARATIONS

Funding

The work was supported by Major Science and Technology Projects in Guizhou Province (Ministry of Science and Technology Major Project [2014] 6024). The funders had no role in study design, data collection and analysis, decision to publish, or preparation of the manuscript.

Grant Disclosures

The following grant information was disclosed by the authors:
Guizhou Province (Ministry of Science and Technology): [2014] 6024.

Competing Interests

The authors declare that they have no competing interests.

Author Contributions

- Xiao Feng conceived and designed the experiments, performed the experiments, analyzed the data, prepared figures and/or tables, and approved the final draft.
- Zhao Yang conceived and designed the experiments, performed the experiments, analyzed the data, prepared figures and/or tables, and approved the final draft.
- Xiurong Wang conceived and designed the experiments, analyzed the data, authored or reviewed drafts of the paper, and approved the final draft.

Data Availability

The following information was supplied regarding data availability:

Data is available as a [Supplemental File](#) and at NCBI: [PRJNA598974](#).

Supplemental Information

Supplemental information for this article can be found online at <http://dx.doi.org/10.7717/peerj.10933#supplemental-information>.

REFERENCES

- Anders S, Huber W. 2012.** *Differential expression of RNA-Seq data at the gene level-the DESeq package*. Heidelberg: European Molecular Biology Laboratory (EMBL).
- Anjum SA, Xie XY, Wang LC, Saleem MF, Man C, Lei W. 2011.** Morphological, physiological and biochemical responses of plants to drought stress. *African Journal of Agricultural Research* **6(9)**:2026–2032.
- Bolger AM, Lohse M, Usadel B. 2014.** Trimmomatic: a flexible trimmer for Illumina sequence data. *Bioinformatics* **2014(30)**:2114–2120 DOI [10.1093/bioinformatics/btu170](#).
- Buchfink B, Xie C, Huson DH. 2015.** Fast and sensitive protein alignment using DIAMOND. *Nature Methods* **12(1)**:59–60 DOI [10.1038/nmeth.3176](#).
- Challabathula D, Zhang Q, Bartels D. 2018.** Protection of photosynthesis in desiccation-tolerant resurrection plants. *Journal of Plant Physiology* **2018(227)**:84–92 DOI [10.1016/j.jplph.2018.05.002](#).
- Chen Y, Li C, Yi J, Yang Y, Lei C, Gong M. 2020.** Transcriptome response to drought, rehydration and re-dehydration in potato. *International Journal of Molecular Sciences* **21(1)**:159 DOI [10.3390/ijms21010159](#).
- Choi DW, Zhu B, Close TJ. 1999.** The barley (*Hordeum vulgare* L.) dehydrin multigene family: sequences, allele types, chromosome assignments, and expression characteristics of 11 Dhn genes of cv Dicktoo. *Theoretical and Applied Genetics* **1999(98)**:1234–1247 DOI [10.1007/s001220051189](#).
- Collett H, Butowt R, Smith J, Farrant J, Illing N. 2003.** Photosynthetic genes are differentially transcribed during the dehydration-rehydration cycle in the resurrection plant, *Xerophyta humilis*. *Journal of Experimental Botany* **2003(54)**:2593–2595 DOI [10.1093/jxb/erg285](#).
- Contreras-Porcia L, Thomas D, Flores V, Correa JA. 2011.** Tolerance to oxidative stress induced by desiccation in *Porphyra columbina* (Bangiales, Rhodophyta). *Journal of Experimental Botany* **62(6)**:1815–1829 DOI [10.1093/jxb/erq364](#).
- Dace H, Sherwin HW, Illing N, Farrant JM. 1998.** Use of metabolic inhibitors to elucidate mechanisms of recovery from desiccation stress in the resurrection plant *Xerophyta humilis*. *Plant Growth Regulation* **1998(24)**:171–177.

- Dalal VK, Tripathy BC. 2018.** Water-stress induced downsizing of light-harvesting antenna complex protects developing rice seedlings from photo-oxidative damage. *Scientific Reports* **2018(8)**:1–16 DOI [10.1038/s41598-017-14419-4](https://doi.org/10.1038/s41598-017-14419-4).
- Deeba F, Pandey AK, Pandey V. 2016.** Organ specific proteomic dissection of Selaginella bryopteris undergoing dehydration and rehydration. *Frontiers in Plant Science* **7(482)**:425 DOI [10.3389/fpls.2016.00425](https://doi.org/10.3389/fpls.2016.00425).
- Demirel U, Morris WL, Ducreux LJM, Yavuz C, Asim A, Tindas I, Campbell R, Morris J, Verrall S, Hedley P, Gokce Z, Caliskan S, Aksoy E, Caliskan M, Taylor M, Hancock RD. 2020.** Physiological, biochemical, and transcriptional responses to single and combined abiotic stress in stress-tolerant and stress-sensitive potato genotypes. *Frontiers in Plant Science* **11**:169 DOI [10.3389/fpls.2020.00169](https://doi.org/10.3389/fpls.2020.00169).
- Din J, Khan SU, Ali I, Gurmani AR. 2011.** Physiological and agronomic response of canola varieties to drought stress. *Journal of Animal and Plant Sciences* **2011(21)**:78–82.
- Dong S, Jiang Y, Dong Y, Wang L, Wang W, Ma Z, Yan C, Ma C, Liu L. 2019.** A study on soybean responses to drought stress and rehydration. *Saudi Journal of Biological Sciences*. **26(8)**:2006–2017 DOI [10.1016/j.sjbs.2019.08.005](https://doi.org/10.1016/j.sjbs.2019.08.005).
- Ernst J, Bar-Joseph Z. 2006.** STEM: a tool for the analysis of short time series gene expression data. *BMC Bioinformatics* **7(1)**:191 DOI [10.1186/1471-2105-7-191](https://doi.org/10.1186/1471-2105-7-191).
- Feng Y, Liang C, Li B, Wan T, Liu T, Cai Y. 2017.** Differential expression profiles and pathways of genes in drought resistant tree species *Prunus mahaleb* roots and leaves in response to drought stress. *Scientia Horticulturae* **2017(226)**:75–84.
- Giannopolitis CN, Ries SK. 1977.** Superoxide dismutases: I. Occurrence in higher plants. *Plant Physiology* **59(2)**:309–314 DOI [10.1104/pp.59.2.309](https://doi.org/10.1104/pp.59.2.309).
- Grabherr MG, Haas BJ, Yassour M, Thompson DA, Amit I, Adiconis X, Fan L, Raychowdhury R, Zeng Q, Chen Z, Mauceli E, Hacohen N, Gnirke A, Rhind N, Palma F, Birren B, Nusbaum C, Lindblad-Toh K, Friedman N, Regev A. 2011.** Trinity: reconstructing a full-length transcriptome without a genome from RNA-Seq data. *Nature Biotechnology* **29(7)**:644–652 DOI [10.1038/nbt.1883](https://doi.org/10.1038/nbt.1883).
- Griffiths CA, Gaff DF, Neale AD. 2014.** Drying without senescence in resurrection plants. *Frontiers in Plant Science* **5**:36 DOI [10.3389/fpls.2014.00036](https://doi.org/10.3389/fpls.2014.00036).
- Guo Y, Zhao S, Zhu C, Chang X, Yue C, Wang Z, Lin Y, Lai Z. 2017.** Identification of drought-responsive miRNAs and physiological characterization of tea plant (*Camellia sinensis* L.) under drought stress. *BMC Plant Biology* **2017(17)**:1–211 DOI [10.1186/s12870-017-1172-6](https://doi.org/10.1186/s12870-017-1172-6).
- Haas JC, Vergara A, Hurry V, Street NR. 2019.** Candidate regulators and target genes of drought stress in needles and roots of Norway spruce. *BioRxiv* **2015**:517151 DOI [10.1101/517151](https://doi.org/10.1101/517151).
- Hand SC, Menze MA, Toner M, Boswell L, Moore D. 2011.** LEA proteins during water stress: not just for plants anymore. *Annual Review of Physiology* **2011(73)**:115–134 DOI [10.1146/annurev-physiol-012110-142203](https://doi.org/10.1146/annurev-physiol-012110-142203).
- Hummel I, Pantin F, Sulpice R, Piques M, Rolland G, Dauzat M, Christophe A, Pervent M, Bouteillé M, Stitt M, Gibon Y, Muller B. 2010.** Arabidopsis plants acclimate to water deficit at low cost through changes of carbon usage: an integrated perspective using growth, metabolite, enzyme, and gene expression analysis. *Plant Physiology* **154(1)**:357–372 DOI [10.1104/pp.110.157008](https://doi.org/10.1104/pp.110.157008).
- Ingram J, Bartels D. 1996.** The molecular basis of dehydration tolerance in plants. *Annual Review of Plant Biology* **47**:377–403.

- Jin J, Zhang H, Kong L, Gao G, Luo J. 2013. PlantTFDB 3.0: a portal for the functional and evolutionary study of plant transcription factors. *Nucleic acids research* **42**(D1):D1182–D1187 DOI 10.1093/nar/gkt1016.
- John SP, Hasenstein KH. 2018. Biochemical responses of the desiccation-tolerant resurrection fern *Pleopeltis polypodioides* to dehydration and rehydration. *Journal of Plant Physiology* **228**:12–18 DOI 10.1016/j.jplph.2018.05.006.
- Krasensky J, Jonak C. 2012. Drought, salt, and temperature stress-induced metabolic rearrangements and regulatory networks. *Journal of Experimental Botany* **63**(4):1593–1608 DOI 10.1093/jxb/err460.
- Kuromori T, Seo M, Shinozaki K. 2018. ABA transport and plant water stress responses. *Trends in Plant Science* **23**(6):513–522 DOI 10.1016/j.tplants.2018.04.001.
- Lamaoui M, Jemo M, Datla R, Bekkaoui F. 2018. Heat and drought stresses in crops and approaches for their mitigation. *Frontiers in Chemistry* **6**:26 DOI 10.3389/fchem.2018.00026.
- Lan Z, Xiaoli W, Peng L, Tingting W, Xingwen W. 2017. Response of *trachycarpus fortunei* seedlings from different provenances to drought stress and drought resistance evaluation. *Journal of Northeast Forestry University* **11**:1 [In Chinese].
- Langfelder P, Horvath S. 2008. WGCNA: an R package for weighted correlation network analysis. *BMC Bioinformatics* **9**(1):559 DOI 10.1186/1471-2105-9-559.
- Langmead B, Salzberg SL. 2012. Fast gapped-read alignment with Bowtie 2. *Nature Methods* **9**(4):357–359 DOI 10.1038/nmeth.1923.
- Le S, Josse J, Husson F. 2008. FactoMineR: an r package for multivariate analysis. *Journal of Statistical Software* **25**(1):1–18 DOI 10.18637/jss.v025.i01.
- Li C, Lin F, An D, Wang W, Huang R. 2017. Genome sequencing and assembly by long reads in plants. *Genes* **9**(1):6 DOI 10.3390/genes9010006.
- Li H, Liu J, Zhang L, Pang T. 2016. Antioxidant responses and photosynthetic behaviors of *Kappaphycus alvarezii* and *Kappaphycus striatum* (Rhodophyta, Solieriaceae) during low temperature stress. *Botanical Studies* **57**:1–9.
- Li X, Liu Q, Feng H, Deng J, Zhang R, Wen J, Dong J, Wang T. 2019a. Dehydrin MtCAS31 promotes autophagic degradation under drought stress. *Autophagy* **16**(5):1–16.
- Li X, Zhang Q, Yang X, Han J, Zhu Z. 2019b. OsANN3, a calcium-dependent lipid binding annexin is a positive regulator of ABA-dependent stress tolerance in rice. *Plant Science* **2019**(284):212–220 DOI 10.1016/j.plantsci.2019.04.019.
- Liu JJ, Wei Z, Li JH. 2014. Effects of copper on leaf membrane structure and root activity of maize seedling. *Botanical Studies* **55**(1):47 DOI 10.1186/s40529-014-0047-5.
- Liu & Tingting. 2018. The relationship between membrane lipids alteration and drought adaptation in leaves of maize seedlings [D]. Chinese Academy of Sciences and Ministry of Education. Available at [https://kns.cnki.net/KCMS/detail/detail.aspx?dbcode=CMFD&dbname=CMFD201802&filename=1018955651.nh&uid=WEEvREcwSljHSldRa1FhcTdnTnhXM3ZPa1RBbCtIbVVzQmt3V0NqK21jST0=\\$9A4hF_YAuvQ5obgVAqNKPCYcEjKensW4IQMovwHtwkF4VYYPoHbKxJw!!&v=MjY2MjhadVpxRnlyblVYckpWRjI2RnJxOUc5ZkpycEViUEISOGVYMUx1eFlTN0RoMVQzcVRyV00xRnJDVVI3cWY=](https://kns.cnki.net/KCMS/detail/detail.aspx?dbcode=CMFD&dbname=CMFD201802&filename=1018955651.nh&uid=WEEvREcwSljHSldRa1FhcTdnTnhXM3ZPa1RBbCtIbVVzQmt3V0NqK21jST0=$9A4hF_YAuvQ5obgVAqNKPCYcEjKensW4IQMovwHtwkF4VYYPoHbKxJw!!&v=MjY2MjhadVpxRnlyblVYckpWRjI2RnJxOUc5ZkpycEViUEISOGVYMUx1eFlTN0RoMVQzcVRyV00xRnJDVVI3cWY=).
- Luo F, Deng X, Liu Y, Yan Y. 2018. Identification of phosphorylation proteins in response to water deficit during wheat flag leaf and grain development. *Botanical Studies* **59**(1):28 DOI 10.1186/s40529-018-0245-7.
- Michaletti A, Naghavi MR, Toorchi M, Zolla L, Rinalducci S. 2018. Metabolomics and proteomics reveal drought-stress responses of leaf tissues from spring-wheat. *Scientific Reports* **8**(1):5710 DOI 10.1038/s41598-018-24012-y.

- Mistry J, Finn RD, Eddy SR, Bateman A, Punta M. 2013. Challenges in homology search: HMMER3 and convergent evolution of coiled-coil regions. *Nucleic Acids Research* 2013(41):e121 DOI 10.1093/nar/gkt263.
- Postiglione AE, Muday GK. 2020. The role of ROS homeostasis in ABA-induced guard cell signaling. *Frontiers in Plant Science* 11:968.
- Rajasekharan R, Nachiappan V. 2010. Fatty acid biosynthesis and regulation in plants. In: *Plant Developmental Biology-Biotechnological Perspectives*. Berlin: Springer, 105–115.
- Rajasheker G, Jawahar G, Jalaja N, Kumar S, Kumari P, Punita L, Karumanchi A, Reddy P, Rathnagiri P, Sreenivasulu N, Kishor P. 2019. Role and regulation of osmolytes and aba interaction in salt and drought stress tolerance. *Plant Signaling Molecules* 2019:417–436.
- Rivas R, Falcão HM, Ribeiro RV, Machado EC, Pimentel C, Santos MG. 2016. Drought tolerance in cowpea species is driven by less sensitivity of leaf gas exchange to water deficit and rapid recovery of photosynthesis after rehydration. *South African Journal of Botany* 103:101–107 DOI 10.1016/j.sajb.2015.08.008.
- Roberts A. 2013. *Ambiguous fragment assignment for high-throughput sequencing experiments[D]*. Berkeley: UC Berkeley.
- Saini LK, Singh N, Pandey GK. 2020. Plant Protein Phosphatase 2C: Critical Negative Regulator of ABA Signaling. In: *Protein Phosphatases and Stress Management in Plants*. Cham: Springer, 83–102.
- Schmittgen TD, Livak KJ. 2008. Analyzing real-time PCR data by the comparative CT method. *Nature Protocols* 3(6):1101–1108 DOI 10.1038/nprot.2008.73.
- Sharma P, Jha AB, Dubey RS, Pessaraki M. 2012. Reactive oxygen species, oxidative damage, and antioxidative defense mechanism in plants under stressful conditions. *Journal of Botany* 2012(1):1–26 DOI 10.1155/2012/217037.
- Showler AT. 2013. Water deficit stress-host plant nutrient accumulations and associations with phytophagous arthropods. *Abiotic Stress-Plant Responses and Applications in Agriculture* 387–410 DOI 10.5772/53125.
- Stocker TF, Qin D, Plattner G-K, Tignor MMB, Allen SK, Boschung J, Nauels A, Xia Y, Bex V, Midgley P. 2014. *Climate change 2013: the physical science basis. contribution of working group i to the fifth assessment report of ipcc the intergovernmental panel on climate change*. Cambridge: Cambridge University Press.
- Takahashi F, Suzuki T, Osakabe Y, Betsuyaku S, Kondo Y, Dohmae N, Fukuda H, Shinozaki K, Shinozaki K. 2018. A small peptide modulates stomatal control via abscisic acid in long-distance signalling. *Nature* 556:235–238.
- Takahashi F, Kuromori T, Urano K, Yamaguchi-Shinozaki K, Shinozaki K. 2020. Drought stress responses and resistance in plants: From cellular responses to long-distance intercellular communication. *Frontiers in Plant Science* 11:556972 DOI 10.3389/fpls.2020.556972.
- Wang K, He J, Zhao Y, Wu T, Zhou X, Ding Y, Kong L, Wang X, Wang Y, Li J, Song C, Wang B, Yang S, Zhu J, Gong Z. 2018. EAR1 negatively regulates ABA signaling by enhancing 2C protein phosphatase activity. *Plant Cell* 30:815–834.
- Xuekui W. 2006. *The principle and technology of plant physiology and biochemistry experiment [M]*. Beijing: Higher Education Press [In Chinese]
- Yao Y-B, Zhang Q, Wang J-S, Shang J-L, Wang Y, Shi J. 2015. Spatiotemporal change of spring drought in southwest china. *Journal of Animal & Plant Sciences* 25:260–269.
- Yu G, Li F, Qin Y, Bo X, Wu Y, Wang S. 2010. GOSemSim: an R package for measuring semantic similarity among GO terms and gene products. *Bioinformatics* 26(7):976–978 DOI 10.1093/bioinformatics/btq064.

- Yu G, Smith DK, Zhu H, Guan Y, Lam TTY. 2017.** ggtree: an R package for visualization and annotation of phylogenetic trees with their covariates and other associated data. *Methods in Ecology and Evolution* **8**:28–36.
- Yu G, Wang LG, Han Y, He QY. 2012.** clusterProfiler: an R package for comparing biological themes among gene clusters. *OmicS: A Journal of Integrative Biology* **16**:284–287.
- Zhang K, Gan SS. 2012.** An abscisic acid-AtNAP transcription factor-SAG113 protein phosphatase 2C regulatory chain for controlling dehydration in senescing Arabidopsis leaves. *Plant Physiology* **158**(2):961–969 DOI [10.1104/pp.111.190876](https://doi.org/10.1104/pp.111.190876).
- Zhang Z, Ali S, Zhang T, Wang W, Xie L. 2020.** Identification, evolutionary and expression analysis of PYL-PP2C-SnRK2s gene families in soybean. *Plants* **9**(10):1356.